analytical chemistry

Article

Cite This: *Anal. Chem.* 2019, 91, 14865−14872

pubs.acs.org/ac

# Isothermal Titration Calorimetry Enables Rapid Characterization of Enzyme Kinetics and Inhibition for the Human Soluble Epoxide Hydrolase

Giancarlo Abis,[†,∥] Raúl Pacheco-Gómez,[‡] Tam T. T. Bui,[†,§] and Maria R Conte*[,†,§]

[†]Randall Centre for Cell and Molecular Biophysics, School of Basic and Medical Biosciences, King's College London, London, SE1 1UL, United Kingdom

[‡]Malvern Panalytical Ltd, Enigma Business Park, Grovewood Road, Malvern, WR14 1XZ, United Kingdom

[§]Centre for Biomolecular Spectroscopy, King's College London, London, SE1 1UL, United Kingdom

Supporting Information

**ABSTRACT:** Isothermal titration calorimetry (ITC) is conventionally used to acquire thermodynamic data for biological interactions. In recent years, ITC has emerged as a powerful tool to characterize enzyme kinetics. In this study, we have adapted a single-injection method (SIM) to study the kinetics of human soluble epoxide hydrolase (hsEH), an enzyme involved in cardiovascular homeostasis, hypertension, nociception, and insulin sensitivity through the metabolism of epoxy-fatty acids (EpFAs). In the SIM method, the rate of reaction is determined by monitoring the thermal power, while the substrate is being depleted, overcoming the need for synthetic substrates and reducing postreaction processing. Our results show that ITC enables the detailed, rapid, and reproducible characterization of the hsEH-mediated hydrolysis of several natural EpFA substrates. Furthermore, we have applied a variant of the single-injection ITC method for the detailed description of enzyme inhibition, proving the power of this approach in the rapid screening and discovery of new hsEH inhibitors using the enzyme's physiological substrates. The methods described herein will enable further studies on EpFAs' metabolism and biology, as well as drug discovery investigations to identify and characterize hsEH inhibitors. This also promises to provide a general approach for the characterization of lipid catalysis, given the challenges that lipid metabolism studies pose to traditional spectroscopic techniques.

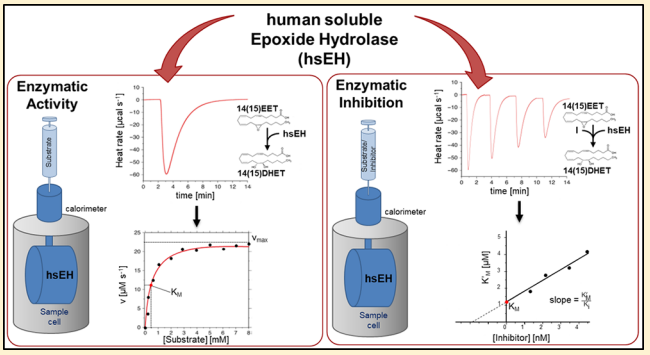


Human soluble epoxide hydrolase (hsEH, EC 3.3.2.10) is a bifunctional enzyme composed of two structurally and functionally independent domains.[1,2] The C-terminal domain (CTD) is responsible for the hydrolysis of numerous epoxy-fatty acids (EpFAs), bioactive epoxidation products of mono- and polyunsaturated fatty acids with essential roles in cellular and organism homeostasis.[2−4] hsEH CTD hydrolyzes EpFAs via an SN2 nucleophilic attack by D335 on the more accessible carbon of the epoxide ring, forming an alkyl-enzyme intermediate, which is then released by the assisted action of D496 and H524.[1,2,5] The catalytic triad is located in the vertex of a large "L-shaped" active site and is surrounded by two hydrophobic surfaces dubbed the W334 niche and the F265 pocket, wherein the aliphatic chains of the EpFAs are accommodated.[1,2,4−6]

The best characterized EpFAs substrates of hsEH CTD are the epoxyeicosatrienoic acids (EETs), epoxy derivatives of arachidonic acid (ARA;[7] Figure S1A). Although four EET regioisomers, namely, 5(6)EET, 8(9)EET, 11(12)EET, and 14(15)EET, have been isolated in several organs,[8] the latter two have been shown to be the predominant ARA epoxidation metabolites.[9] EETs function primarily as endothelial-derived hyperpolarizing factors in the cardiovascular system and kidneys.[7] They play a role in vasorelaxation and vascular homeostasis, exerting anti-inflammatory and pro-angiogenic actions.[7] The bioavailability of EETs is reduced by hsEH-mediated hydrolysis of their epoxy ring to generate the corresponding vicinal diols, namely, dihydroxyeicosatrienoic acids (DHETs; Figure S1A), which possess a considerably reduced biological activity.[7]

In addition to EETs, hsEH hydrolyzes several bioactive epoxy derivatives of linoleic acid (LA) and α-linoleic acid (ALA), including α- and γ-epoxyoctadecadienoic acids (α/γ-EpODEs), epoxyeicosatetraenoic acids (EpETEs), epoxydocosapentaenoic acids (EpDPEs), and epoxyoctadecaenoic acids (EpOMEs;[10,11] Figure S1B). The physiological role of α- and γ-EpODEs is yet unknown, although their hydrolysis products, the γ-dihydroxy-octadecadienoic acids (γ-DiHODE), exhibit a

**Received:** April 16, 2019
**Accepted:** October 29, 2019
**Published:** October 29, 2019




DOI: 10.1021/acs.analchem.9b01847
*Anal. Chem.* 2019, 91, 14865−14872

moderate positive inotropic effect.[12] EpETEs and EpDPEs show a similar breadth of activities to EETs.[13] Vasodilation, antithrombotic, antiangiogenic, and anti-inflammatory effects have been ascribed to both EpETEs and EpDPEs, as well as diminished tumor growth and metastasis in murine models.[10,14,15] Interestingly, the hsEH-mediated hydrolysis product of 19(20)EpDPE, namely, the 19(20)-dihydroxy-docosapentaenoic acid (19(20)DiHDPE), accumulates in the retinas and vitreous humor of diabetic retinopathy patients, as a result of increased expression levels of the enzyme, and aggravates disease severity by altering the localization of cholesterol-binding proteins in the cell membrane and leading to a breakdown of endothelial barrier function.[16]

Contrary to the largely beneficial physiological effects ascribed to other EpFAs, 9(10)- and 12(13)EpOMEs inhibit mitochondrial respiration in various tissues, leading to cardiotoxicity, renal failure, and adult respiratory distress syndrome,[17,18] albeit cytotoxicity is significantly increased in their sEH-catalyzed products, the dihydroxy-octadecaenoic acids (DiHOMEs).[17]

Interestingly, a liquid chromatography tandem mass spectrometry (LC-MS/MS) study revealed that hsEH displays a different hydrolytic efficiency toward its various EpFA substrates.[10] Although this work provided a first assessment of catalytic profiles for several epoxy fatty acids, potential drawbacks of this methodological approach include the following: (i) it is a discontinuous method, with potentially non-negligible experimental errors; (ii) it requires several sample manipulation steps that could lead to reproducibility issues; (iii) it is time-consuming, technically challenging, and expensive. Herein, we present an isothermal titration calorimetry (ITC)-based method for the systematic characterization of hsEH catalytic efficiency toward its EpFAs substrates. By measuring the intrinsic heat of hsEH-mediated hydrolysis of the epoxy-fatty acids in a continuous manner,[19−23] our method circumvents the limiting issue of the lack of physicochemical properties of EpFAs substrates/products that can be monitored in real time in a continuous manner.[19−23] This new ITC application shows promise in the complete and highly reproducible characterization of hsEH-mediated catalysis of epoxy-fatty acids, with relatively low sample amounts, low costs, and rapid acquisition times.

The second goal of our study was to establish an easy and versatile method to measure inhibition properties of sEH antagonists against natural substrates. Given that dihydroxy-fatty acids generated by hsEH exhibit either cytotoxic effects or reduced biological activity compared to their epoxy precursors, pharmacological inhibition of hsEH has emerged as an extremely appealing therapeutic strategy to increase EpFAs bioavailability and reap their beneficial properties.[24−26] Currently, screening of hsEH inhibitors is mostly performed via a high-throughput spectrofluorimetric assay,[27,28] a fast, economical and highly convenient method that nonetheless carries the main drawback of not employing physiological substrates. To address this, we have adapted an ITC method developed by Di Trani et al.[21] Using a well-known hsEH antagonist as a model system, we demonstrate here that this technique holds promise for the quantitative screening of new hsEH inhibitors using endogenous EpFAs substrates.

## EXPERIMENTAL SECTION

**Enzyme, Substrate, and Inhibitor Sample Preparation.** Recombinant hsEH CTD was obtained as described.[29] This was shown to be necessary and sufficient for EpFA catalysis and to retain the same kinetic profile as full length protein.[29] Protein, EpFAs substrates, and inhibitor AUDA (12-[[(tricyclo[3.3.1.13,7]dec-1-ylamino)carbonyl]amino]-dodecanoic acid) were prepared as reported in the Supporting Information.

**Single-Injection ITC Kinetics Measurements.** The theoretical basis of kinetic measurements by ITC has been described,[19,22,30,31] and details are given in the Supporting Information. Briefly, in a single injection ITC experiment, the total heat measured is proportional to the apparent enthalpy ($\Delta H_{app}$), and the number of moles of product generated. The reaction rate can be related to the amount of heat generated over time. From the derived Michaelis−Menten plots, the affinity for the substrate ($K_M$), turnover rate ($k_{cat}$), and catalytic efficiency ($k_{cat}/K_M = K_{sp}$) values can be obtained.

Experiments were performed on MicroCal PEAQ-ITC and MicroCal iTC200 calorimeters (Malvern). An hsEH CTD solution at 250 nM was placed in the sample cell, and a 0.5−1.5 mM substrate solution was loaded in the injection syringe. One single 38 $\mu$L injection was performed with a speed of 0.58−0.76 $\mu$L s$^{-1}$. Controls were carried out as described in the Supporting Information. Apparent enthalpy of the reaction, heat rate ($dQ/dt$), and Michaelis−Menten plots were generated using MicroCal PEAQ-ITC Analysis Software (Malvern).

**Progressive Inhibition ITC Enzyme Kinetics Measurements.** A solution containing 0.5 mM of 14(15)EET and 67.37 nM of AUDA was injected into the cell containing 250 nM of hsEH CTD. Four 9.5 $\mu$L injections of 12.5 s each were performed at a speed of 0.76 $\mu$L s$^{-1}$. Control experiments are described in the Supporting Information. Apparent reaction enthalpy, $dQ/dt$ rates, and Michaelis−Menten parameters were generated using the MicroCal PEAQ-ITC Analysis Software (Malvern). Apparent $K_M$ values ($K_M'$) were obtained,[32] and data fitting in GraphPad provided the $K_M'/K_i$ ratio,[20,21] where $K_i$ is the inhibition constant.

**Inhibitory Constant Measurements with a Spectrofluorometric Method.** AUDA inhibitory potency was tested with a spectrofluorometric method,[28] detailed in the Supporting Information.

## RESULTS

**A Single-Injection ITC Method Characterizes the Kinetics of hsEH CTD-Mediated Hydrolysis of 14(15)EET.** To probe the kinetics of EpFA hydrolysis catalyzed by hsEH CTD, we employed an ITC single-injection method (SIM).[22,23] The substrate solution in the syringe of the calorimeter was injected in a single step into the sample cell containing the enzyme solution, producing a heat response which endured for as long as the reaction proceeds, returning to the baseline when the reaction reached completion and all the substrate had been transformed into product. Rapid catalyses give rise to narrow peaks, while slow catalyses generate broad peaks. Whereas the total area of the peak depends on the amount of substrate injected and the apparent enthalpy of the reaction, its shape is governed by enzyme concentration, Michaelis−Menten parameters, rate of substrate injection, and intrinsic calorimeter response.[19,21]

14(15)EET, the *par excellence* EpFA substrate of hsEH,[8] was used as a test compound to demonstrate method applicability and to set up the experimental conditions for this study. Optimization included varying concentrations of substrate and



DOI: 10.1021/acs.analchem.9b01847
Anal. Chem. 2019, 91, 14865−14872

enzyme, as well as reference power, injection speed, and spacing. The curve obtained by injecting 14(15)EET into a solution of hsEH CTD was negative, narrow, and deep, indicating a fast reaction (Figure 1A). The $\Delta H_{app}$ was

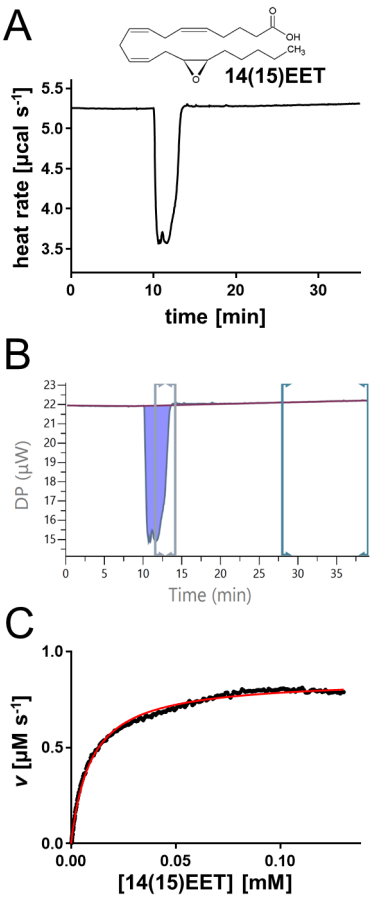


**Figure 1.** Quantitative characterization of hsEH-mediated hydrolysis of 14(15)EET. (A) Representative thermal profile of a single-injection of 14(15)EET into hsEH CTD. (B) Screenshot from the MicroCal PEAQ-ITC analysis software. The $\Delta H_{app}$ was calculated by integrating the area under the peak (violet), upon definition of the baseline through manual adjustments of the left markers workspace (green). The data points used for the Michaelis–Menten kinetics curve fitting were obtained by manual adjustments of the right markers workspace (gray), selecting the window between the end of the injection (maximum substrate concentration – saturating enzyme conditions) and the end of the decaying portion of the peak (minimum substrate concentration – beginning of the kinetics curve). Note that the first part of the curve corresponding to substrate injection was not included in the rate plot analysis. (C) Representative Michaelis–Menten fit of the $\{[S]_i;v_i\}$ data point extrapolated from B using the MicroCal PEAQ-ITC analysis software analysis.

calculated by integrating the area under the peak, and the Michaelis–Menten kinetics curve fitting was obtained by manually selecting the window between the end of the injection (maximum substrate concentration, corresponding to saturating enzyme conditions) and the end of the decaying portion of the injection (minimum substrate concentration, corresponding to the beginning of the kinetics curve; Figure 1B). The software fitting calculates $\{[S]_i;v_i\}$ data points through eqs 2 and 3 (Supporting Information), building a Michaelis–Menten curve (Figure 1C), thereby providing $k_{cat}$ and $K_M$ values. The catalytic efficiency ($K_{sp}$) was manually calculated as the $k_{cat}/K_M$ ratio. In the optimal conditions, these experiments gave a $k_{cat}$ of 6.64 ± 1.54 $s^{-1}$ and a $K_M$ of 12.88 ± 1.94 $\mu$M for the hsEH-mediated hydrolysis of 14(15)EET (Table 1). To assess any product inhibition effect, the $\Delta H_{app}$ of two subsequent injections was compared: no significant variation was observed (Figure S2A and B), demonstrating an absence of product inhibition for this hsEH CTD-mediated hydrolysis reaction.

**Kinetic Characterization of hsEH CTD-Mediated Hydrolysis of All EETs.** The experimental method and conditions optimized for 14(15)EET were applied to analyze the hsEH CTD-catalyzed hydrolysis of the other regioisomeric EETs. Thermal profiles and Michaelis–Menten parameters significantly differed (Table 1). The hydrolysis of 5(6)EET generated a very small and broad peak (Figure 2A), indicating a low $\Delta H_{app}$. Although it was possible to extrapolate a $k_{cat}$ value of 0.35 ± 0.05 $s^{-1}$ and a $K_M$ of 46.61 ± 10.98 $\mu$M, the error associated with this measurement was considerably greater than for the other EETs, due to the reduced magnitude of the heat response and the inability to reach enzyme saturation.[23] Attempts to perform the experiments with higher substrate concentration in fact resulted in precipitation of the mixture. The experiment with 8(9)EET and 11(12)EET gave a $k_{cat}$ of 1.28 ± 0.19 $s^{-1}$ and a $K_M$ of 23.10 ± 2.39 $\mu$M for the former and a $k_{cat}$ of 4.31 ± 0.16 $s^{-1}$ and a $K_M$ of 1.74 ± 0.20 $\mu$M for the latter. Control experiments to check for substrate autohydrolysis and product inhibition are reported in Figures S2B and S3.

**Kinetic Characterization of hsEH CTD-Mediated Hydrolysis of n-3 and n-6 EpFAs.** Beyond the EETs, the enzymatic activity of hsEH toward other EpFAs was measured by ITC. We selected two EpETEs, one EpDPE and one EpOME, to cover the chemical scaffold diversity of hsEH substrates. Though belonging to the same chemical class, 8(9)EpETE and 17(18)EpETE exhibited different enthalpy and kinetic values (Figure 3A and B, Table 1). The turnover rate for the 8(9)EpETE was 1.61 ± 0.01 $s^{-1}$, significantly higher than for the 17(18)-regioisomer (0.64 ± 0.06 $s^{-1}$), and its $K_M$ (9.74 ± 0.13 $\mu$M) was almost 3 times lower than 17(18)EpETE (26.37 ± 4.05 $\mu$M). A broad negative peak in the thermal profile was also obtained for 19(20)EpDPE, indicating a slow hsEH CTD-mediated hydrolysis (Figure 3C) described by a turnover rate of 1.62 ± 0.08 $\mu$M and a $K_M$ of 26.60 ± 1.21 $\mu$M (Table 1). The hydrolysis of 12(13)EpOME gave rise to a narrow heat flow profile (Figure 3D), similar to the ones observed for 11(12)- and 14(15)EET, with a $k_{cat}$ of 9.65 ± 0.19 $s^{-1}$ and a $K_M$ of 2.98 ± 0.56 $\mu$M. As observed with the other substrates, negligible heat and product inhibition effects were observed in blank test injections (Figures S2B and S4).

**Characterization of hsEH CTD Inhibition Using ITC.** We adapted a protocol that builds on SIM ITC enzyme kinetic measurements[21] to set up a versatile and continuous method to measure the inhibitory potency of hsEH antagonists against natural substrates, as well as readily characterize their mode of inhibition. We evaluated the thermal power of 14(15)EET hydrolysis in the presence of the well-known hsEH inhibitor AUDA. The enzyme was placed in the calorimeter cell, while the syringe was loaded with a mixture of substrate and inhibitor. A series of injections was then performed (Figure 4A). In the experiment, AUDA accumulated in the sample cell with its concentration increasing 1-fold with each successive


DOI: 10.1021/acs.analchem.9b01847
Anal. Chem. 2019, 91, 14865–14872

**Table 1. Mean and Standard Error Values for the Apparent Enthalpy and Kinetics Parameters of hsEH CTD-Mediated Hydrolysis of the EpFAs Analyzed in This Study**[a]

| substrate | $\Delta H_{app}$ [kJ mol$^{-1}$] | $k_{cat}$ [s$^{-1}$] | $K_M$ [$\mu$M] | $K_{sp}$ [s$^{-1}$ $\mu$M$^{-1}$] |
|---|---|---|---|---|
| 5(6)EET | −4.84 ± 0.65 | 0.35 ± 0.05 | 46.61 ± 10.98 | 0.01 ± 0.001 |
| 8(9)EET | −39.45 ± 3.88 | 1.28 ± 0.19 | 23.10 ± 2.39 | 0.054 ± 0.010 |
| 11(12)EET | −12.43 ± 0.62 | 4.31 ± 0.16 | 1.74 ± 0.20 | 2.53 ± 0.25 |
| 14(15)EET | −23.72 ± 3.46 | 6.64 ± 1.54 | 12.88 ± 1.94 | 0.527 ± 0.075 |
| 8(9)EpETE | −34.13 ± 0.93 | 1.61 ± 0.01 | 9.74 ± 0.13 | 0.173 ± 0.006 |
| 17(18)EpETE | −51.78 ± 1.73 | 0.64 ± 0.06 | 26.37 ± 4.05 | 0.025 ± 0.003 |
| 19(20)EpDPE | −23.73 ± 1.82 | 1.62 ± 0.08 | 26.60 ± 1.21 | 0.061 ± 0.003 |
| 12(13)EpOME | −5.67 ± 0.38 | 9.65 ± 0.19 | 2.98 ± 0.56 | 3.56 ± 0.86 |

[a]The values were obtained as described in the methods.

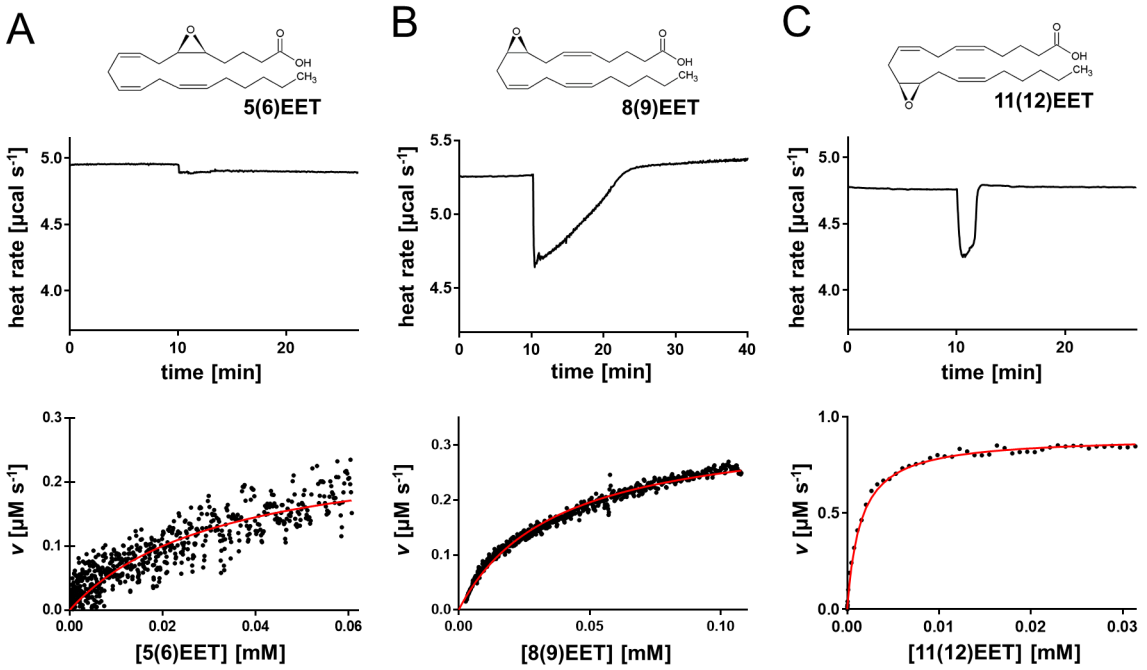


**Figure 2.** Single-injection isotherms and data fitting for the hsEH-mediated hydrolysis of EETs. Experiments are shown for (A) 5(6)EET, (B) 8(9)EET, and (C) 11(12)EET. Each panel reports a representative thermal profile of a single-injection experiment (top plot) and the corresponding data fit using the Michaelis−Menten model (bottom plot). Note that the faster the reaction, the fewer data points will be available for fitting the plot.

injection. This results in each injection producing a heat flow response that was progressively lower and broader than the preceding one, owing to increased hsEH CTD inhibition. Blank test injections showed little heat effects of substrate/inhibitor dilution into the buffer (Figure S5A). Each peak injection was analyzed individually to measure the $\Delta H_{app}$ and extract the Michaelis−Menten parameters. The $k_{cat}$ values derived from each peak were identical (8.89 ± 1.64 s$^{-1}$) and in agreement with the value detected in the absence of inhibitor (Table 1). The apparent $K_M$ ($K_M'$) for 14(15)EET increased at every successive injection with growing inhibitor concentration (Figure 4B). The $k_{cat}$ and $K_M'$ values obtained by this analysis indicate a model of competitive inhibition,[32] which is consistent with AUDA's reported mode of action.[26,33] As AUDA is a competitive inhibitor, the $y$-intercept of the $K_M'$ vs AUDA concentration plot (Figure 4B) provides the true $K_M$,[32] measured as 11.91 ± 3.43 $\mu$M, in concurrence with the value for the 14(15)EET substrate obtained in the absence of inhibitor (Table 1). The analysis of the slope of the straight line fitted to the data points gives the $K_M'/K_i$ ratio,[32] providing an average $K_i$ for AUDA of 7.62 ± 2.81 nM. This is in excellent agreement with the value obtained from a spectrofluorimetric assay using the synthetic substrate PHOME[28,29,34] (Figure S6A and B).

## DISCUSSION

The study of EpFA catalysis mediated by hsEH is severely limited by the unavailability of fast, simple, and effective methods to study their kinetics of hydrolysis. The only technique available thus far is a LC-MS/MS-based methodology,[10] which, although highly sensitive, is a postreaction ancillary technique, involving multiple steps of sample manipulation and analysis,[32] and requiring highly specialized equipment and technical expertise. To develop a truly general, versatile, and rapid enzyme kinetics assay, we have developed a single-injection ITC (SIM) approach. By detecting the heat released or absorbed in real time during catalysis, this technique follows reactions of native substrates without the need of detectable changes in physicochemical properties to track the concentration of substrate or product over time. The single-injection ITC method yields both thermodynamic and kinetic parameters in a single experiment. Recent advances in


DOI: 10.1021/acs.analchem.9b01847
Anal. Chem. 2019, 91, 14865−14872

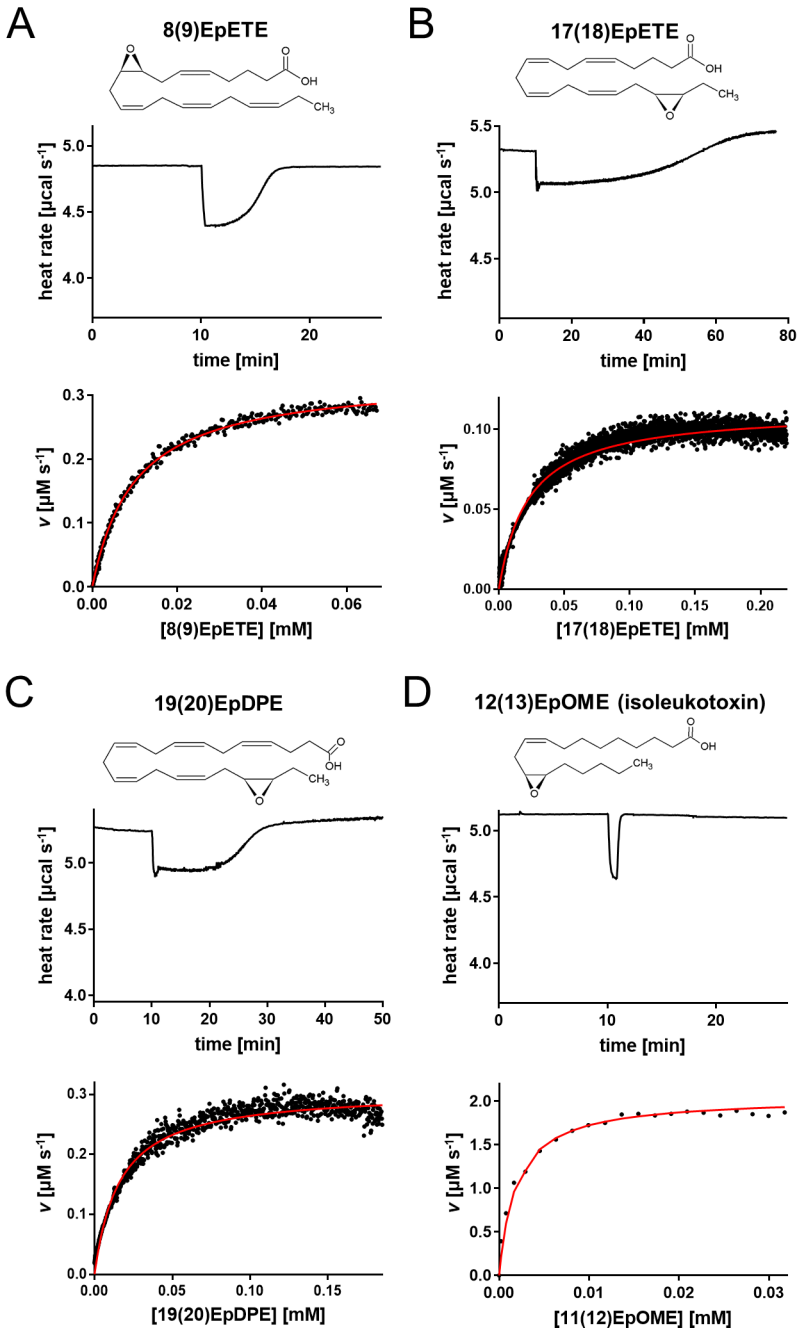


**Figure 3.** Single-injection isotherms and data fitting for the hsEH-mediated hydrolysis of EpFAs. Experiments are shown for (A) 8(9)EpETE, (B) 17(18)EpETE, (C) 19(20)EpDPE, and (D) 12(13)EpOME. Each panel reports a representative thermal profile of a single-injection experiment (top plot) and the corresponding data fit using the Michaelis−Menten model (bottom plot). Note that for faster reactions, fewer data points will be available for fitting the plot.

instrumentation, faster response times, and analysis software (*e.g.* the new PEAQ-ITC analysis software) have allowed this approach to become more user-friendly and routine. Compared to the multi-injection ITC method counterpart, the SIM is significantly faster, requires less enzyme, and is less subject to errors linked to baseline drift, or other time-dependent effects, including enzyme aggregation and/or precipitation and substrate degradation,[19] because of the reduced experimental time and faster data acquisition.[19,30]

The ITC single-injection application presented here enables the rapid characterization of kinetic parameters of various natural EpFA substrates of hsEH, such as EETs, EpETEs, EpDPEs, and EpOMEs, using small amounts of protein and substrate, with each experiment taking on an average 50 min (including washing and preparation of the instrument). To our knowledge, this is the first example of the ITC SIM applied to lipid catalysis, and it is the only method to date that allows a quantitative analysis of hsEH-mediated hydrolysis of EpFAs in a continuous manner.

Our investigations revealed that all EpFAs tested could be hydrolyzed by hsEH, albeit significant differences were observed in their kinetics profiles, in agreement with a previous study.[10] It is noteworthy that although data fitted well to the Michaelis−Menten model, hsEH CTD performs a two-step



DOI: 10.1021/acs.analchem.9b01847
*Anal. Chem.* 2019, 91, 14865−14872

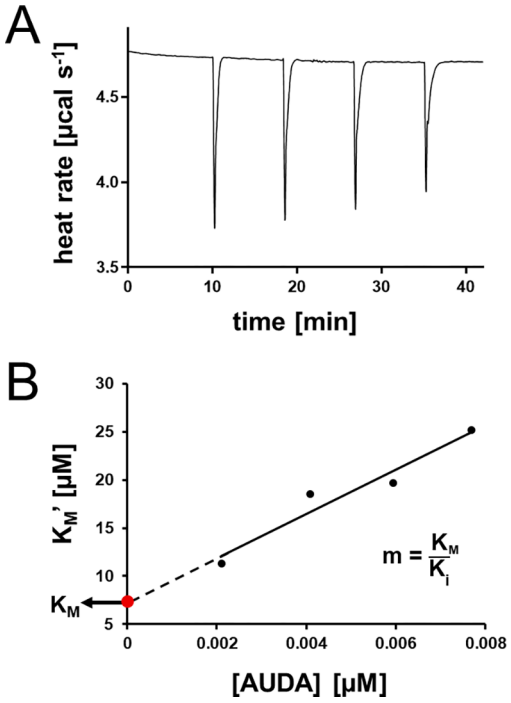


**Figure 4.** hsEH CTD inhibition studies. (A) Representative thermal power of 14(15)EET/AUDA injections into hsEH CTD. The magnitude of the peaks decreases with each successive injection due to the increased concentration of the inhibitor, while the slope of the recovery increased, suggesting a competitive mode of inhibition. (B) Linear $K_M'$ vs AUDA concentration fitting from data shown in A.

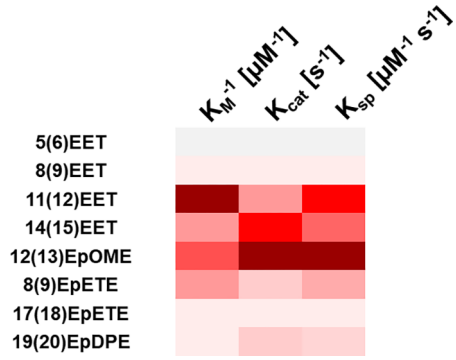


**Figure 5.** Heatmap of the kinetics parameters of the hsEH CTD-mediated hydrolysis of EpFAs showing $K_{sp}$ inverse of $K_M$ ($K_M^{-1}$ [$\mu M^{-1}$]) and $k_{cat}$. Colors span from gray to dark red with increasing values. Each shade of gray-to-red indicates an increase of the 12.5th percentile of the total interval of values. A combination of dark red shades indicates high affinity, turnover rate, and efficiency.

catalysis, undergoing first the formation of a covalent enzyme–substrate alkyl intermediate followed by its hydrolysis.[4,35] In these cases, $K_M$ values describe the concentration of the substrate for which the catalytic rate is half maximal, instead of providing an accurate measure of the substrate affinity for the enzyme,[36] and $k_{cat}$ values represent mainly the hydrolysis rate of the covalent intermediate, given that this second step of the hsEH CTD-mediated catalysis is at least an order of magnitude slower than the first (formation of the alkyl covalent intermediate).[4,35]

Our results (Table 1) indicate that $K_M$ and $k_{cat}$ values vary significantly depending on the chemical scaffold and the epoxide position on the fatty acid structure. Whereas variations of $K_M$ values could not easily be correlated with substrate properties in this study, in general $k_{cat}$ values were the largest when the epoxide was central, on the carbon positions 11, 12, and 14 of the fatty acid chain. Comparison of catalytic efficiency ($K_{sp}$), a measurement of the overall rate of the reaction and specificity of an enzyme for a substrate,[36] revealed the preferred EpFA targets for hsEH CTD, summarized in a heatmap (Figure 5). For the substrates tested in our study, the rank order of hsEH CTD catalytic preference is 12(13)EpOME > 11(12)EET > 14(15)EET > 8(9)EpETE > 19(20)EpDPE ≈ 8(9)EET > 17(18)EpETE > 5(6)EET. A trend is revealed here, correlating catalytic efficiency with the position of the epoxide function: hsEH CTD distinctly prefers epoxides located in the middle of the fatty acid chain, at positions 11, 12, and 14, with its activity steadily decreasing for substrates bearing the epoxide moiety closer to either the carboxyl acid group or to the methyl group at the end of the hydrocarbon chain. Having the epoxide close to the carboxyl function is the least preferred configuration, as indicated by the lowest efficiency for 5(6)EET. This appears consistent with the narrow "L-shaped" hsEH CTD active site, with the catalytic triad positioned deep in the vertex and surrounded by two large hydrophobic regions.[1,6] Notably, the overall substrate preference for sEH revealed by ITC is largely in agreement with what was previously observed in Morisseau et al.[10] by LC-MS/MS, although it is noteworthy that the discrete Michaelis–Menten parameters do differ in the two studies (especially $k_{cat}$).

Given that hsEH inhibition is a potential therapeutic approach in a number of pathological conditions, detailed knowledge of hsEH catalytic efficiency toward its various substrates is of great importance, as it will inform on how such an inhibition will affect the metabolism of several EpFAs, enabling the prediction of the expected outcome from their altered levels. As the relative abundance of each epoxy-fatty acid varies within the organism,[10,13] a pharmacological intervention may have simultaneous assorted responses in different tissues and organs.

In addition to measuring the kinetics of catalysis for different EpFA targets of hsEH, we also devised an ITC method to screen new hsEH inhibitors using natural substrates. Our ITC application brings significant advantages. First, it evaluates inhibitor potency using hsEH physiological substrates, circumventing the problems associated with employing non-native fluorogenic compounds. This will have a particular bearing for the analysis of noncompetitive and mixed inhibitors, which bind respectively to the enzyme–substrate complex or to both the enzyme and substrate.[32] Interestingly, new allosteric inhibitors of hsEH have started to emerge,[34] increasing the timely relevance of this new methodology. Furthermore, as the efficacy of noncompetitive and mixed inhibitors may in principle differ from substrate to substrate, our ITC method offers a well-suited solution for a systematic characterization of inhibition versus a battery of EpFA substrates. As a second major benefit, the ITC method allows for a straightforward characterization of the mode of inhibition (*i.e.*, competitive, uncompetitive or noncompetitive/mixed),[32] which is critical to drug development as evaluating the inhibitory power, given that it reveals the nature of the inhibited state(s).



DOI: 10.1021/acs.analchem.9b01847
*Anal. Chem.* 2019, 91, 14865–14872

## CONCLUSIONS

Despite the crucial biological roles of hsEH in a variety of physiological and pathological states, a comprehensive understanding of its catalytic activity against a compendium of natural substrates remains inadequate. Equally, the availability of assays that characterize and screen hsEH inhibitors using native substrates has been limited to date. We have presented a novel, versatile, expedient, and reliable ITC SIM application that has the potential to be adopted as the method of choice to perform such characterizations. Being not reliant on specific physicochemical and spectroscopic properties, our method is ideally posed to facilitate the discovery of new putative epoxy substrates of hsEH. Moreover, calorimetric measurements can be performed in mixtures and suspensions, *e.g.*, in cellular and crude tissue extracts, as well as allowing measurements over a range of biologically relevant conditions[19,37] (pH, redox conditions, salt concentration etc.), thereby having the potential to contribute to advances of hsEH biology in health and disease. As recent discoveries suggest a role for hsEH in redox regulatory systems,[38,39,34] our newly developed ITC method can be used to assess the impact of the enzyme oxidative state on both catalysis and inhibition of EpFAs hydrolysis.

Taken together, our results show the first proof-of-concept for kinetic characterization and inhibitor screening of hsEH activities using ITC, an approach which is generally applicable to other enzymes involved in lipid metabolism, and should help in the search for novel inhibitors of this important class of enzymes.

## ASSOCIATED CONTENT

### Supporting Information

The Supporting Information is available free of charge on the ACS Publications website at DOI: 10.1021/acs.analchem.9b01847.

Seven figures and one table reporting a schematic of the EpFAs metabolism, all the experimental controls, and the spectrofluorimetric analysis of hsEH CTD inhibition as well as full experimental procedures and protocols, as well as a full mathematical treatment of the theoretical basis of kinetic rates determination by ITC (PDF)

## AUTHOR INFORMATION


### Corresponding Author

*E-mail: sasi.conte@kcl.ac.uk.

### ORCID

Giancarlo Abis: 0000-0003-1440-7832
Raúl Pacheco-Gómez: 0000-0001-6932-9734
Tam T. T. Bui: 0000-0002-8074-4928
Maria R Conte: 0000-0001-8558-2051

### Present Address

[‖]Division of Bioscience, Institute of Structural and Molecular Biology, University College London, London, WC1E 6BT, UK


### Author Contributions

M.R.C., G.A., and R.P.-G. contributed to the planning and the design of the study. G.A. prepared the recombinant enzyme used in all the experiments and performed the spectrofluorometric analysis. G.A., R.P.-G., and M.R.C. optimized the experimental setup for the ITC kinetics analysis. G.A. and T.T.T.B. performed the ITC experiments for both kinetics and inhibition studies. M.R.C., G.A., and R.P.-G. participated in the data analysis and contributed to the writing of the manuscript. M.R.C. obtained funding for this work.

### Notes

The authors declare no competing financial interest.

## ACKNOWLEDGMENTS

G.A. was supported by a BHF interdisciplinary Ph.D. studentship and a pump priming award from the BHF Centre of Excellence, King's College London. G.A. and M.R.C. thank Malvern Panalytical Ltd., particularly Maria Walton for the logistic support and Peter Gimeson for the help with the experimental setting and data analysis. The authors thank the Centre for Biomolecular Spectroscopy funded by the Wellcome Trust and British Heart Foundation (ref 202767/Z/16/Z and IG/16/2/32273, respectively).

## REFERENCES


(1) Argiriadi, M.; Morisseau, C.; Hammock, B. D.; Christianson, D. W. *Proc. Natl. Acad. Sci. U. S. A.* **1999**, *96*, 10637−10642.
(2) Gomez, G. A.; Morisseau, C.; Hammock, B. D.; Christianson, D. W. *Biochemistry* **2004**, *43*, 4716−4723.
(3) Borhan, B.; Jones, D. A.; Pinot, F.; Grant, D. F.; Kurth, M. J.; Hammock, B. D. *J. Biol. Chem.* **1995**, *270* (45), 26923−26930.
(4) Morisseau, C.; Hammock, B. D. *Annu. Rev. Pharmacol. Toxicol.* **2005**, *45* (1), 311−333.
(5) Argiriadi, M. A.; Morisseau, C.; Goodrow, M. H.; Dowdy, D. L.; Hammock, B. D.; Christianson, D. W. *J. Biol. Chem.* **2000**, *275* (20), 15265−15270.
(6) Gomez, G. A.; Morisseau, C.; Hammock, B. D.; Christianson, D. W. *Protein Sci.* **2006**, *15*, 58−64.
(7) Imig, J. D. *Physiol. Rev.* **2012**, *92* (1), 101−130.
(8) Spector, A. A.; Fang, X.; Snyder, G. D.; Weintraub, N. L. *Prog. Lipid Res.* **2004**, *43* (1), 55−90.
(9) Capdevila, J. H.; Falck, J. R.; Harris, R. C. *J. Lipid Res.* **2000**, *41*, 163−181.
(10) Morisseau, C.; Inceoglu, B.; Schmelzer, K.; Tsai, H.-J.; Jinks, S. L.; Hegedus, C. M.; Hammock, B. D. *J. Lipid Res.* **2010**, *51* (12), 3481−3490.
(11) Gabbs, M.; Leng, S.; Devassy, J. G.; Monirujjaman, M.; Aukema, H. M. *Adv. Nutr.* **2015**, *6* (5), 513−540.
(12) Mitchell, L. A.; Grant, D. F.; Melchert, R. B.; Petty, N. M.; Kennedy, R. H. *Cardiovasc. Toxicol.* **2002**, *2* (3), 219−229.
(13) Gabbs, M.; Leng, S.; Devassy, J. G.; Monirujjaman, M.; Aukema, H. M. *Adv. Nutr.* **2015**, *6* (5), 513−540.
(14) Zhang, G.; Panigrahy, D.; Mahakian, L. M.; Yang, J.; Liu, J.-Y.; Lee, K. S. S.; Wettersten, H. I.; Ulu, A.; Hu, X.; Tam, S.; Hwang, S. H.; Ingham, E. S.; Kieran, M. W.; Weiss, R. H.; Ferrara, K. W.; Hammock, B. D. *Proc. Natl. Acad. Sci. U. S. A.* **2013**, *110* (16), 6530−6535.
(15) Ulu, A.; Harris, T. R.; Morisseau, C.; Miyabe, C.; Inoue, H.; Schuster, G.; Dong, H.; Iosif, A.-M.; Liu, J.-Y.; Weiss, R. H.; Chiamvimonvat, N.; Imig, J. D.; Hammock, B. D. *J. Cardiovasc. Pharmacol.* **2013**, *62* (3), 285−297.
(16) Hu, J.; Dziumbla, S.; Lin, J.; Bibli, S.; Zukunft, S.; de Mos, J.; Awwad, K.; Frömel, T.; Jungmann, A.; Devraj, K.; Cheng, Z.; Wang, L.; Fauser, S.; Eberhart, C. G.; Sodhi, A.; Hammock, B. D.; Liebner, S.; Müller, O. J.; Glaubitz, C.; Hammes, H. P.; Popp, R.; Fleming, I. *Nature* **2017**, *552*, 248−252.
(17) Moran, J. H.; Weise, R.; Schnellmann, R. G.; Freeman, J. P.; Grant, D. F. *Toxicol. Appl. Pharmacol.* **1997**, *146* (1), 53−59.
(18) El-Sherbeni, A. A.; El-Kadi, A. O. S. *Arch. Toxicol.* **2014**, *88* (11), 2013−2032.
(19) Mazzei, L.; Ciurli, S.; Zambelli, B. *Isothermal Titration Calorimetry to Characterize Enzymatic Reactions*; Elsevier Inc., 2016; vol. *1*, p 567, DOI: 10.1016/bs.mie.2015.07.022.
(20) Di Trani, J. M.; Moitessier, N.; Mittermaier, A. K. *Anal. Chem.* **2017**, *89* (13), 7022−7030.




DOI: 10.1021/acs.analchem.9b01847
*Anal. Chem.* 2019, 91, 14865−14872

(21) Di Trani, J. M.; Moitessier, N.; Mittermaier, A. K. *Anal. Chem.* **2018**, *90* (14), 8430−8435.
(22) Todd, M. J.; Gomez, J. *Anal. Biochem.* **2001**, *296* (2), 179−187.
(23) Transtrum, M. K.; Hansen, L. D.; Quinn, C. *Methods* **2015**, *76*, 194−200.
(24) Wagner, K. M.; McReynolds, C. B.; Schmidt, W. K.; Hammock, B. D. *Pharmacol. Ther.* **2017**, *180*, 62−76.
(25) Imig, J.; Hammock, B. *Nat. Rev. Drug Discovery* **2009**, *8* (10), 794−805.
(26) Shen, H. C.; Hammock, B. D. *J. Med. Chem.* **2012**, *55* (5), 1789−1808.
(27) Morisseau, C.; Hammock, B. D. Measurement of soluble epoxide hydrolase (sEH) activity. *Current Protocols in Toxicology*; Wiley & Sons, Inc.: Hoboken, NJ, 2007; Chapter 4, pp 4.23.1−4.23.18,
(28) Wolf, N. M.; Morisseau, C.; Jones, P. D.; Hock, B.; Hammock, B. D. *Anal. Biochem.* **2006**, *355*, 71−80.
(29) Abis, G.; Charles, R. L.; Eaton, P.; Conte, M. R. *Protein Expression Purif.* **2019**, *153*, 105−113.
(30) Hansen, L. D.; Transtrum, M. K.; Quinn, C.; Demarse, N. *Biochim. Biophys. Acta, Gen. Subj.* **2016**, *1860* (5), 957−966.
(31) Luo, Q.; Chen, D.; Boom, R. M.; Janssen, A. E. M. *Food Chem.* **2018**, *268* (June), 94−100.
(32) Copeland, R. A. *Evaluation of Enzyme Inhibitors in Drug Discovery*; Wiley, 2005.
(33) Kim, I.; Morisseau, C.; Watanabe, T.; Hammock, B. D. *J. Med. Chem.* **2004**, *47* (8), 2110−2122.
(34) Abis, G.; Charles, R. L.; Kopec, J.; Yue, W. W.; Atkinson, R. A.; Bui, T. T. T.; Lynham, S.; Popova, S.; Sun, Y.-B.; Fraternali, F.; Eaton, P.; Conte, M. R. *Commun. Biol.* **2019**, *2*, 188.
(35) Hopmann, K. H.; Himo, F. *J. Phys. Chem. B* **2006**, *110* (42), 21299−21310.
(36) Price, N. C.; Stevens, L. *Fundamentals of Enzymology*; Oxford University Press, 1999.
(37) Freyer, M. W.; Lewis, E. A. *Methods Cell Biol.* **2008**, *84*, 79−113.
(38) Charles, R. L.; Burgoyne, J. R.; Mayr, M.; Weldon, S. M.; Hubner, N.; Dong, H.; Morisseau, C.; Hammock, B. D.; Landar, A.; Eaton, P. *Circ. Res.* **2011**, *108* (3), 324−334.
(39) Charles, R. L.; Rudyk, O.; Prysyazhna, O.; Kamynina, A.; Yang, J.; Morisseau, C.; Hammock, B. D.; Freeman, B. a; Eaton, P. *Proc. Natl. Acad. Sci. U. S. A.* **2014**, *111* (22), 8167−8172.



DOI: 10.1021/acs.analchem.9b01847
*Anal. Chem.* 2019, 91, 14865−14872